

Nuclear Data Research at RPI

Report to CSEWG 2016

Y. Danon, E. Liu, E. Blain, B. McDermott, K. Ramic, C. Wendorff
Gaerttner LINAC Center, Rensselaer Polytechnic Institute, Troy, NY, 12180
and

D. Barry, R. Block, J. Burke, A. Daskalakis, B. Epping, G. Leinweber, M. Rapp, T. Trumbull
Naval Nuclear Laboratory, KAPL, P.O. Box 1072, Schenectady, NY 12301



CSEWG meeting, November 14, 2016 at BNL

Completed and Planned Measurements

- **Completed Measurements**

- **Capture**

- ^{56}Fe - 500 eV - 500 keV, 45m flight path

- **Scattering**

- Zr <0.5 MeV, preliminary data shown

- **Planned measurements**

- **Scattering**

- Zr - for $E < 0.5$ MeV, continue development
 - Hf or Cu for $0.5 \text{ MeV} < E < 20 \text{ MeV}$

- **Transmission**

- Hf – for $0.5 \text{ MeV} < E < 20 \text{ MeV}$
 - Ta – RRR and URR

- **Photoneutrons**

- Be, Ta – measurements with 20-60 MeV bremsstrahlung

- **Capture**

- Ta – RRR (URR completed)

Data Analysis

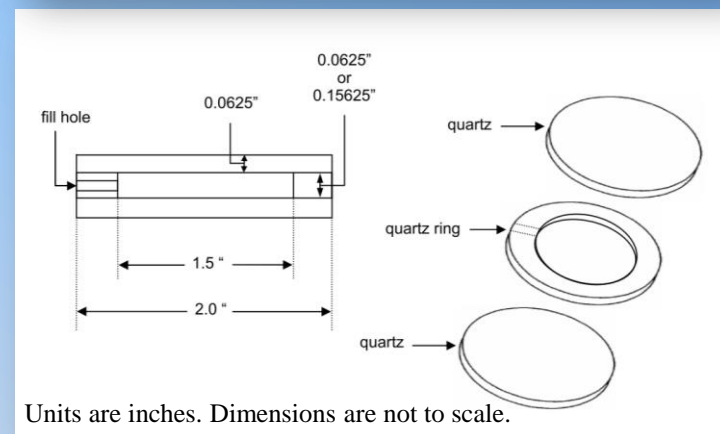
Measure	Sample	Status
High Energy 0.5 – 20 MeV	Ti, Ta, Zr, ⁵⁶ Fe, W, Cu, Pb	Transmission, Internal report completed. Transmission, Internal report in progress.
RRR and URR Transmission and Capture	Cs, Fe, Ta Rh, Re ¹⁶⁴ Dy ^{161,162,163,164} Dy ²³⁶ U ^{92/94,95,96,98,100,nat} Mo Ta	Resonance analysis in progress. Internal report completed. Accepted for publication in Progress in Nuclear Energy. Manuscript was submitted for publication. Published in Progress in Nuclear Energy 86, Pages 11–17, Jan. 2016. ⁹⁶ Mo - Analysis is ongoing (⁹⁵ Mo URR – Published in Phys. Rev. C). URR publication in final internal review.
Scattering	Fe Pb	Publication in progress Internal report completed
Thermal Scattering	H ₂ O, polyethylene, quartz	Analysis in progress

Resonance Region Measurements



^{164}Dy Resonance Region Measurements

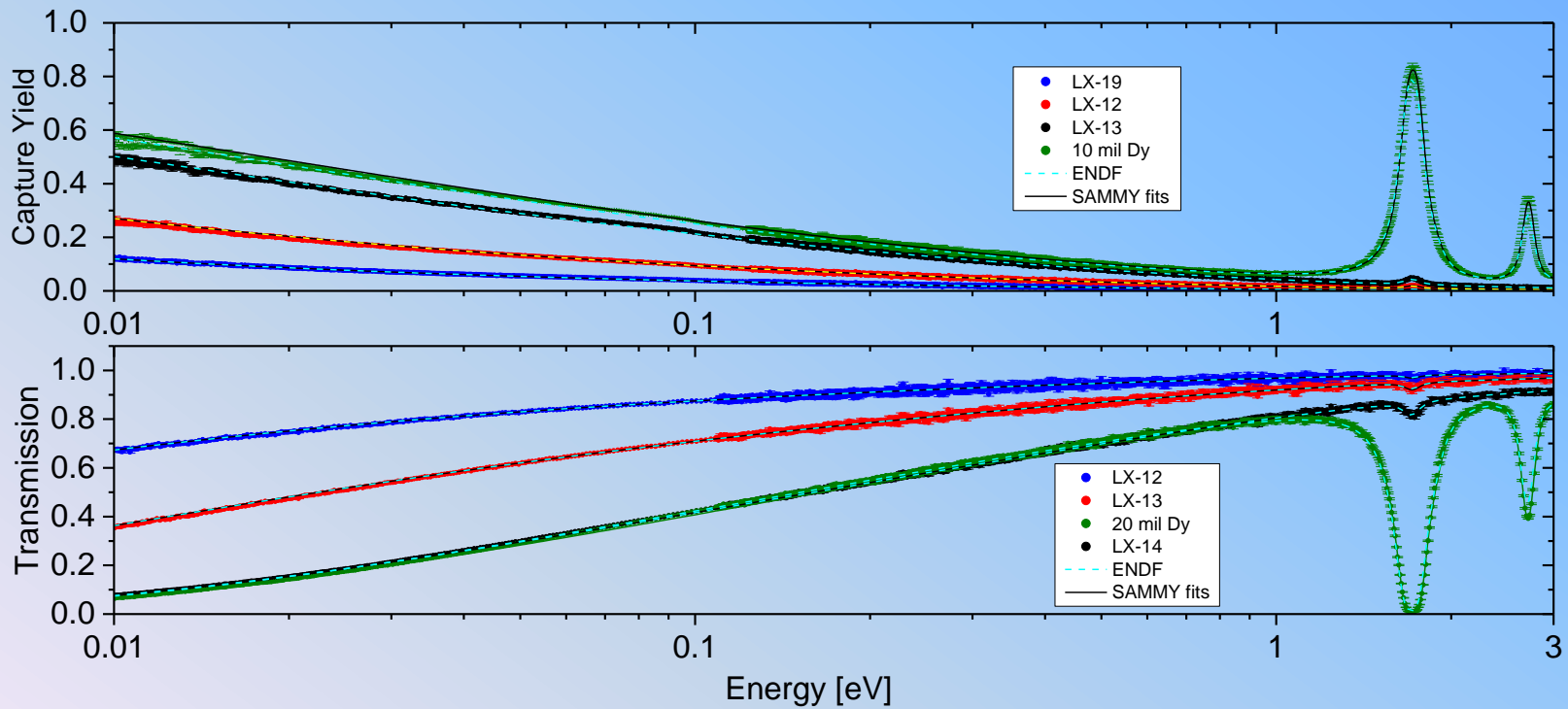
- Enriched ^{164}Dy and elemental samples measured
- Dy solutions in quartz cells used to ensure uniformity in thin samples
 - Equivalent of 0.0254 mm enriched metal
 - Thin and uniform
 - Diluted in D_2O
- The strong 5.44 eV resonance in ^{162}Dy was used for capture flux normalization



Thermal ^{164}Dy Measurements

^{164}Dy Thermal Total Cross Section	
NNL/RPI	ENDF
2980 ± 10 barns	2981 barns

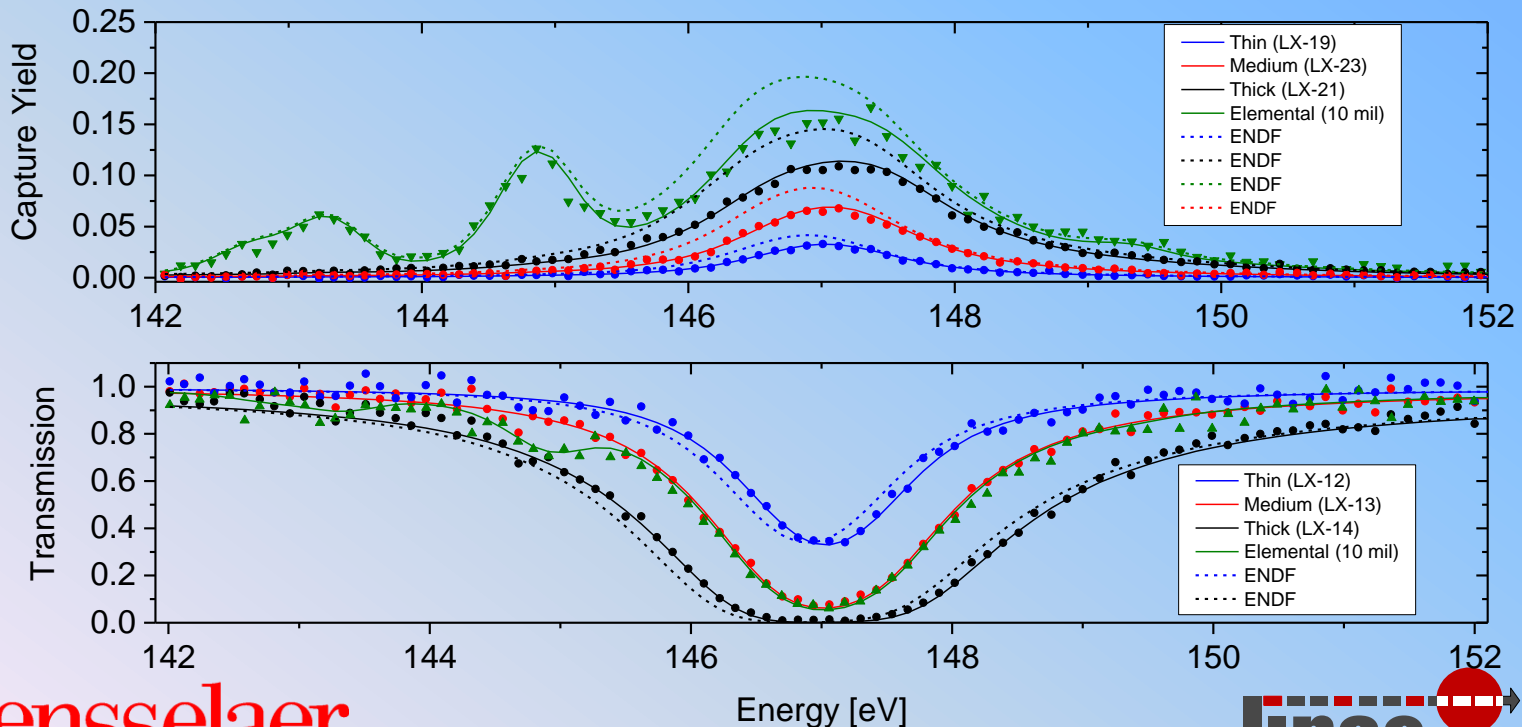
^{164}Dy Capture Resonance Integral	
NNL/RPI	ENDF
338 ± 1 barns	342.2 barns



^{164}Dy Resonance at 147 eV

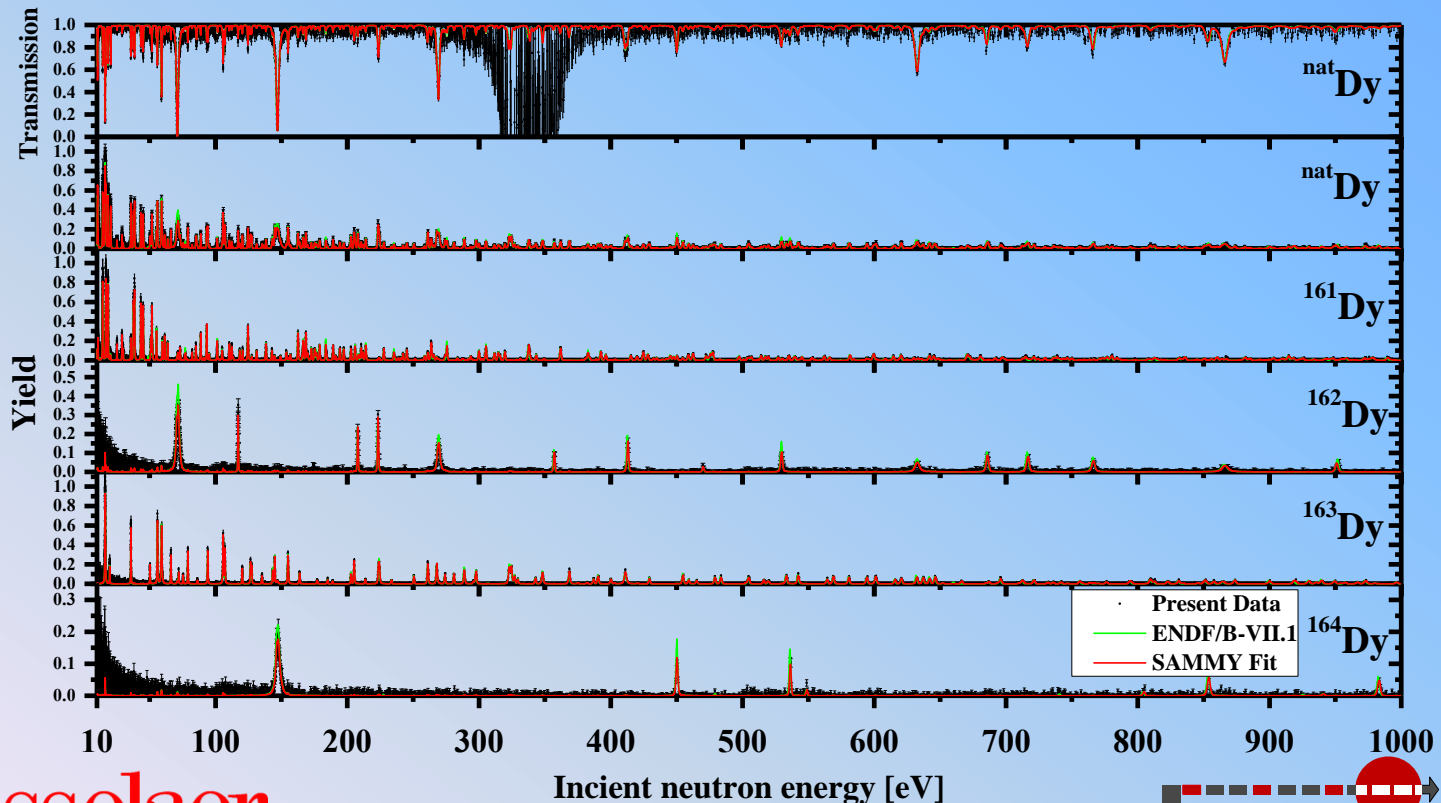
- Lowest positive energy and strongest resonance in ^{164}Dy
- Γ_n within uncertainties of ENDF, but Γ_γ lower, as seen in capture fits

Source	E_0 (eV)	$\Delta E_{o,B}$ (eV)	$\Delta E_{o,ext}$ (eV)	Γ_γ (meV)	$\Delta\Gamma_{\gamma,B}$ (meV)	$\Delta\Gamma_{\gamma,ext}$ (meV)	Γ_n (meV)	$\Delta\Gamma_{n,B}$ (meV)	$\Delta\Gamma_{n,ext}$ (meV)	Iso- tope	J
NNL/RPI	147.105	0.005	0.008	86	2	1	830	8	10	164	0.5
ENDF/B-VII.1	147.97			114.2			820			164	0.5



$^{161,162,163,164}\text{Dy}$ Capture Measurements

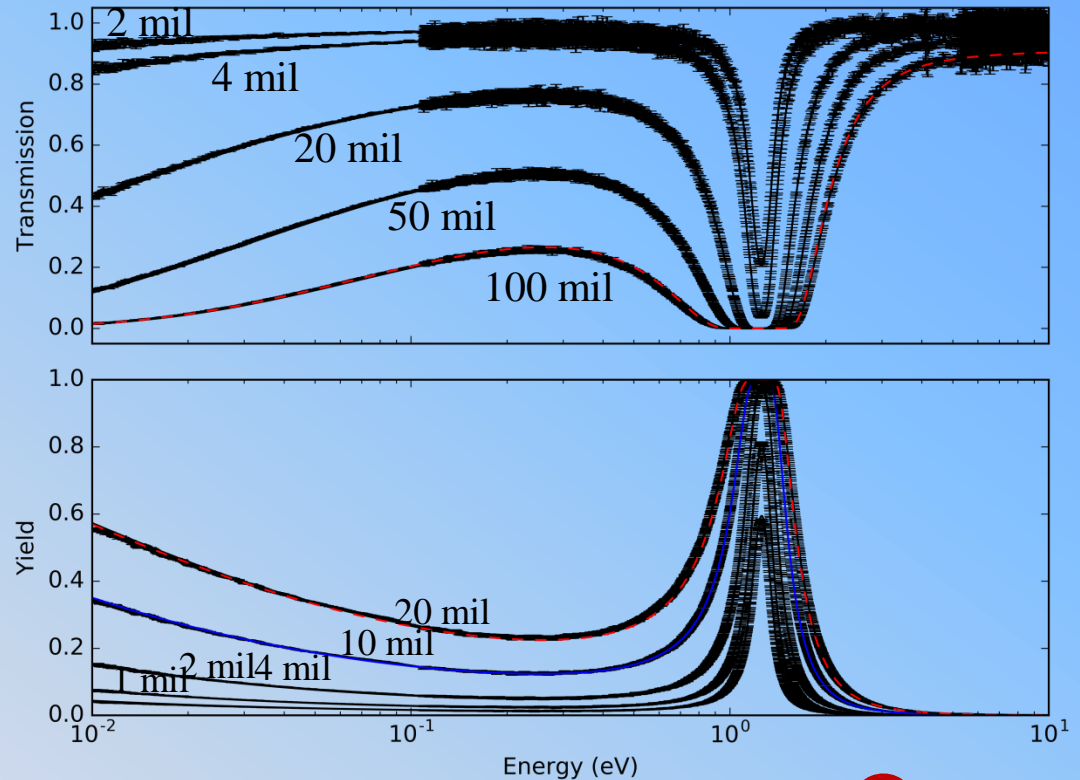
- Publication is in final review and includes all resonance parameters
- New resonances: 29 in ^{161}Dy , 17 in ^{163}Dy .
- ENDF/B-VII.1 resonances not observed: 6 in ^{161}Dy isotope, 2 in ^{163}Dy , 4 in ^{164}Dy .
- $^{\text{nat}}\text{Dy}$ resonance integral was found to be 1405 ± 3.5 , $\sim 0.3\%$ higher than ENDF/B-VII.1



Rh Transmission and Capture in the RRR

Thermal cross section (barns)			
	Total	Capture	Elastic
NNL	149 ± 1	144 ± 1	5.2 ± 0.1
ENDF/B-VII.1	146.3	142	4.3

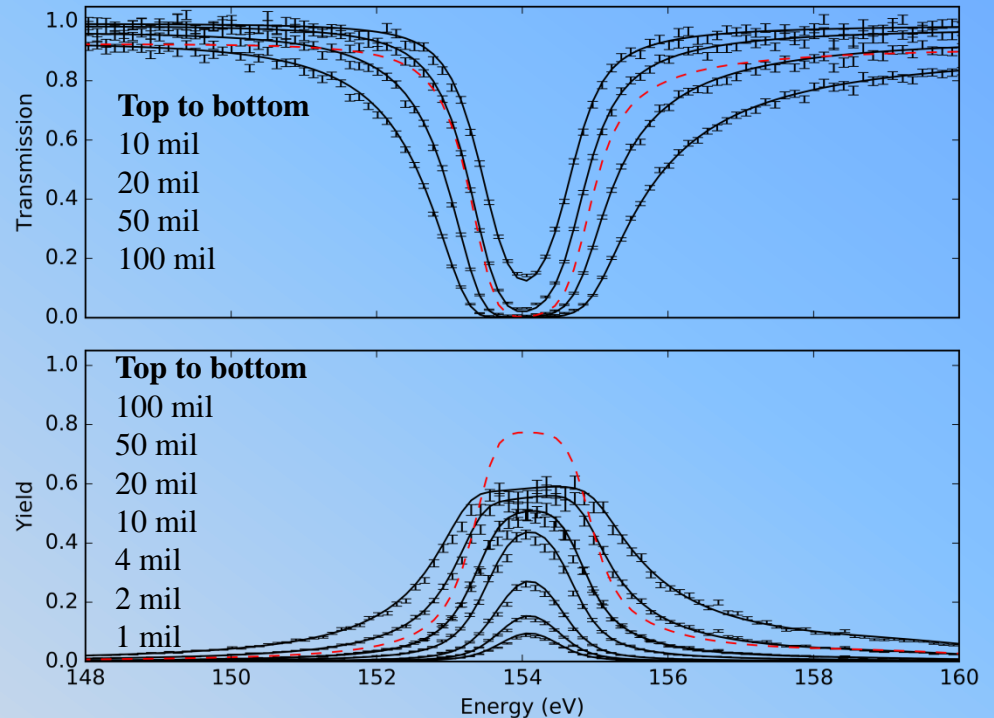
- Measured multiple sample thicknesses in both transmission and capture
 - Transmission at ~ 15 m flight path
 - Capture at ~ 25 m flight path
- Capture slightly higher than ENDF/B-VII.1
- Scattering $\sim 20\%$ higher than ENDF/B-VII.
 - small cross section compared to capture



Rh Transmission and Capture in the RRR

Resonance Integral (barns)			
	Total	Capture	Elastic
NNL	1120 ± 10	990 ± 10	121 ± 1
ENDF-7.1	1084	968	108

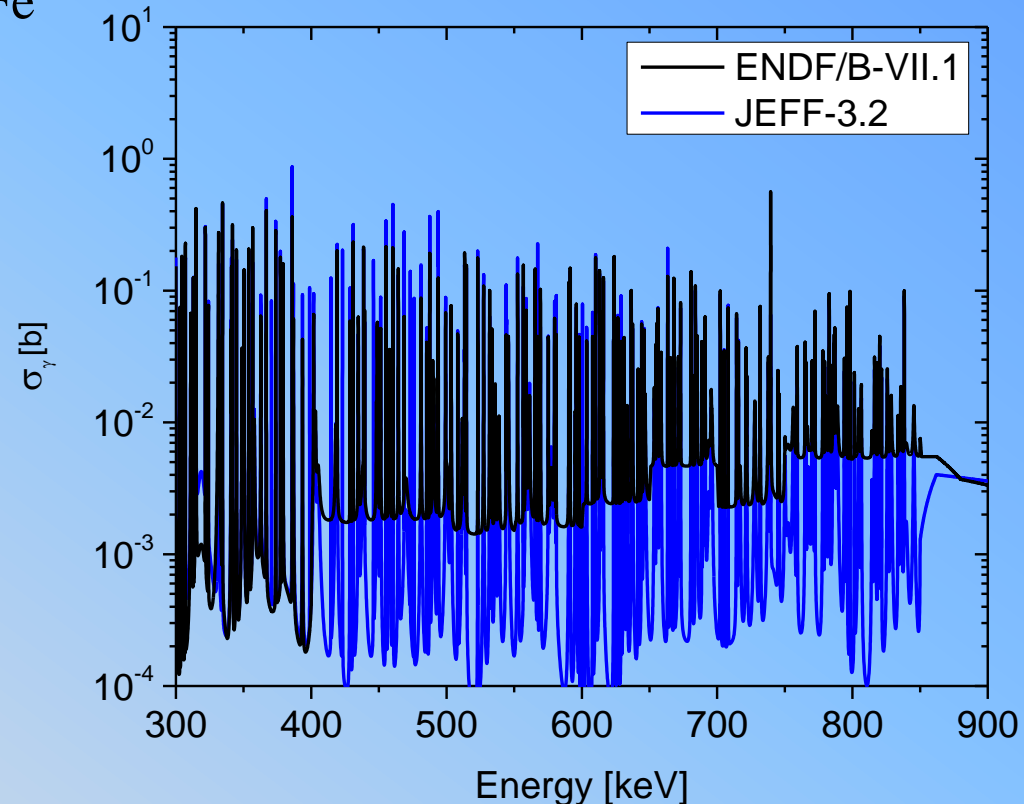
- Measured multiple sample thicknesses in both transmission and capture
 - Both Transmission and Capture at ~ 25 m flight path
- The absorption resonance integral is $\sim 3\%$ higher compared to ENDF/B-VII.1
- Scattering resonance integral is $\sim 12\%$ higher compared to ENDF/B-VII.1



Example of a large difference compared to ENDF/B-VII.1

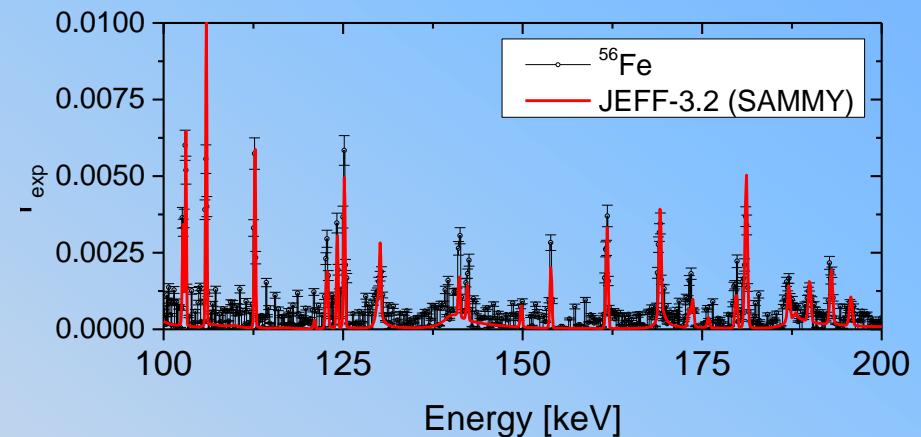
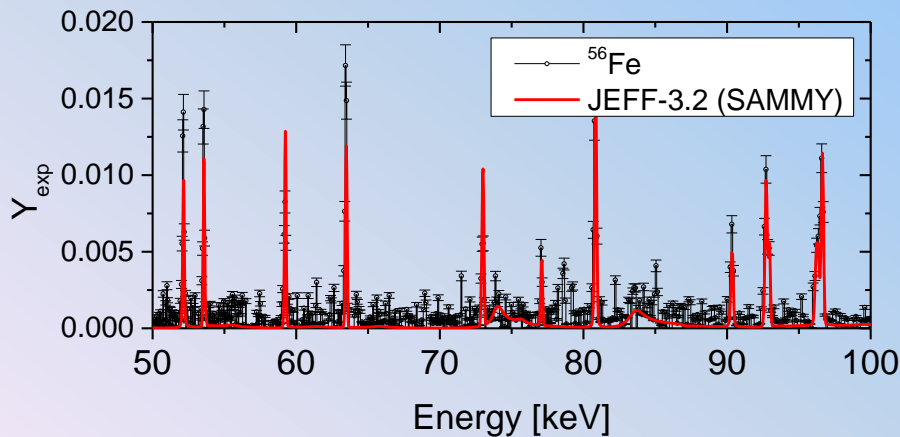
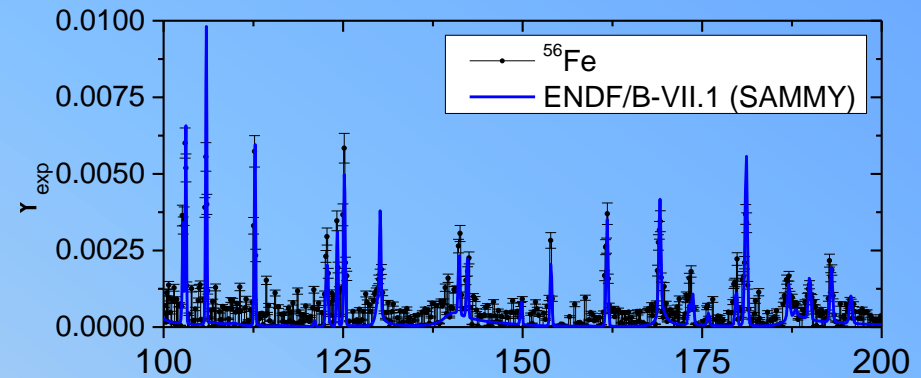
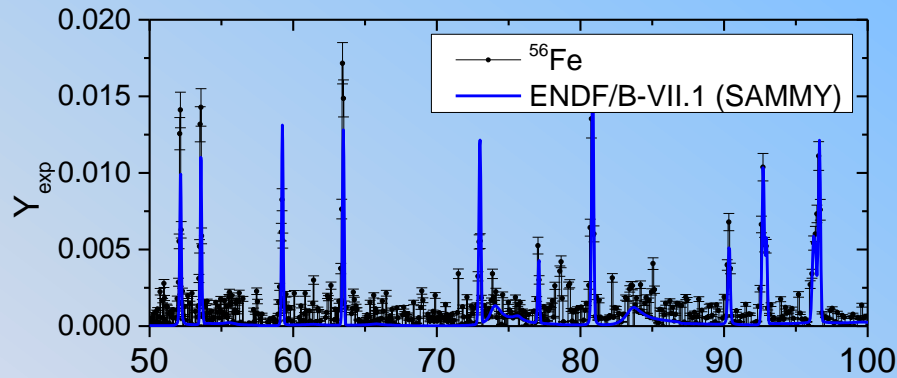
New measurements of ^{56}Fe capture cross section up to 2 MeV

- ENDF/B-VII.1 evaluation for ^{56}Fe has artificial background above 400 keV
- Discrepancies are apparent in MCNP calculations
- Used C_6D_6 detector array for capture measurements



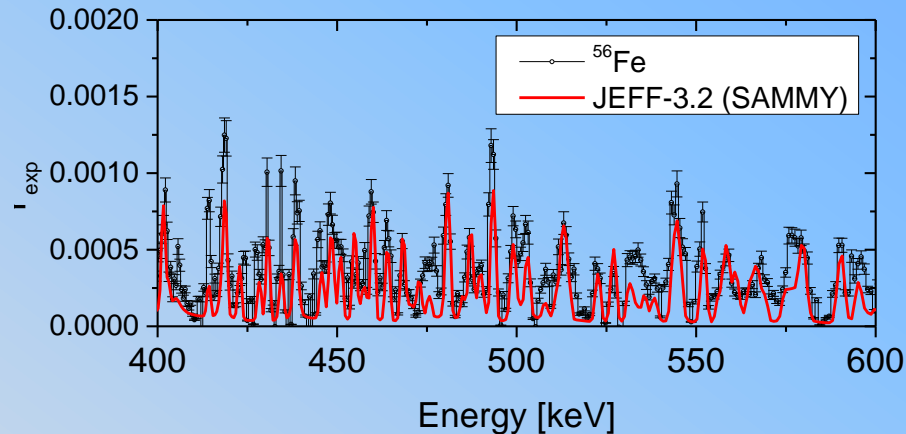
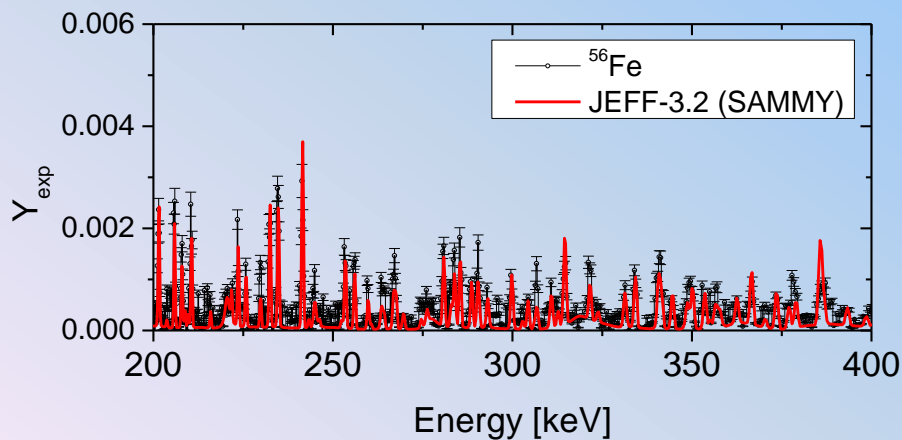
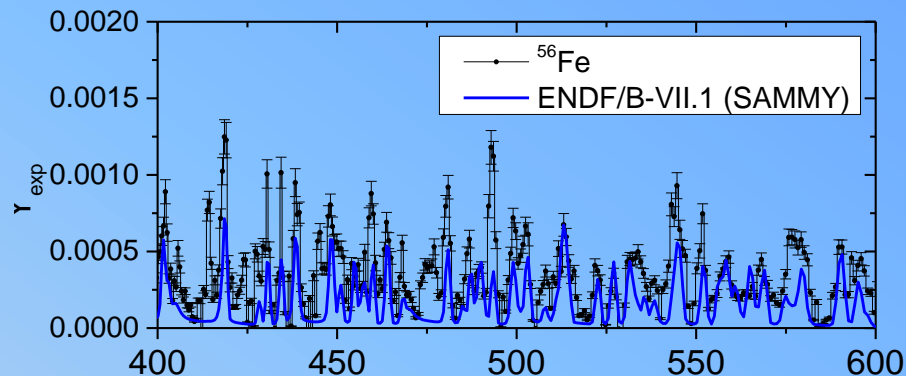
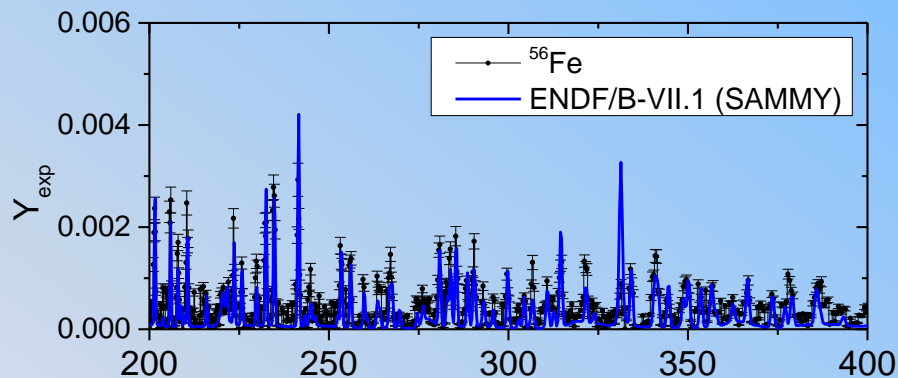
^{56}Fe Results – SAMMY Comparison 50 – 200 keV

- Measured capture yield for ^{56}Fe from 50-200 keV.
- Differences from evaluations are noticeable on some resonances



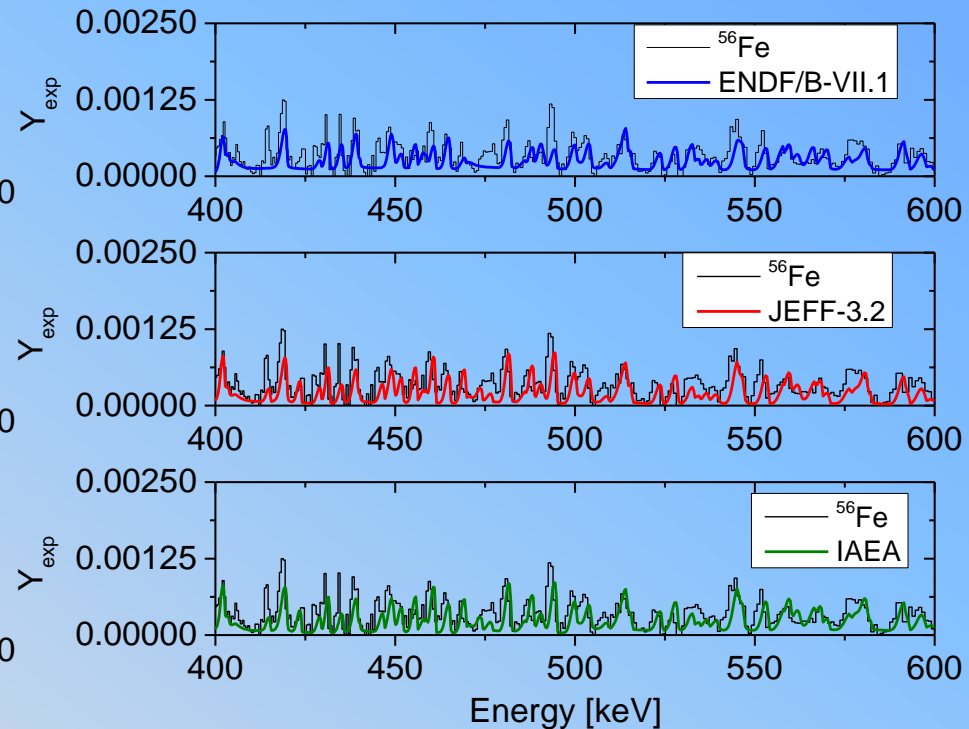
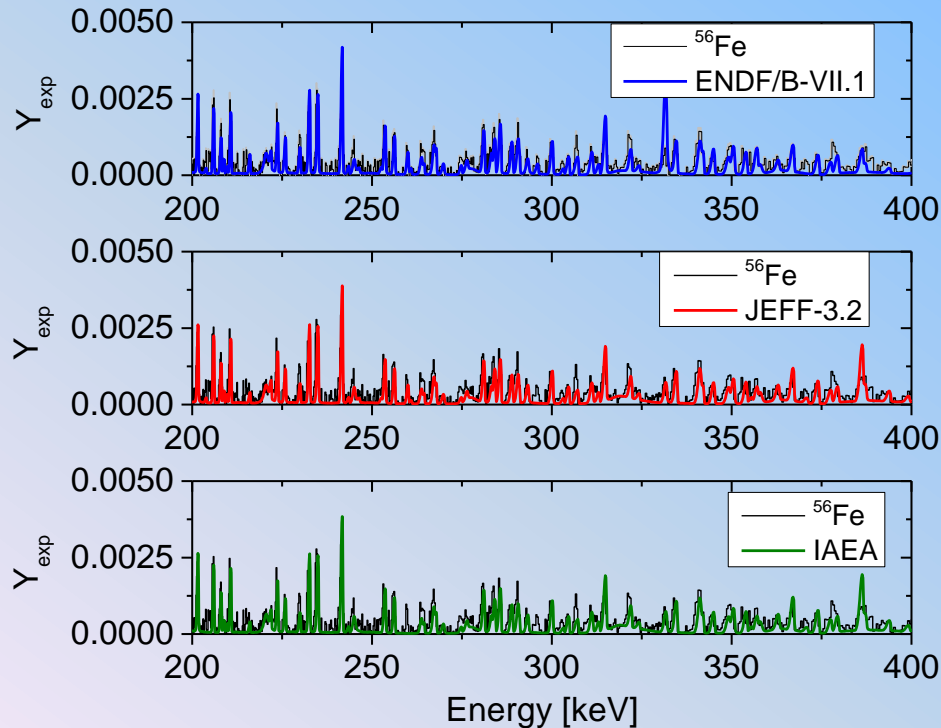
^{56}Fe Results – SAMMY Comparison 200 -600 keV

- Capture yield from 200-400 keV
- Improved signal-to-background at higher energies
- Differences are larger above 400 keV (Experiment is generally higher)



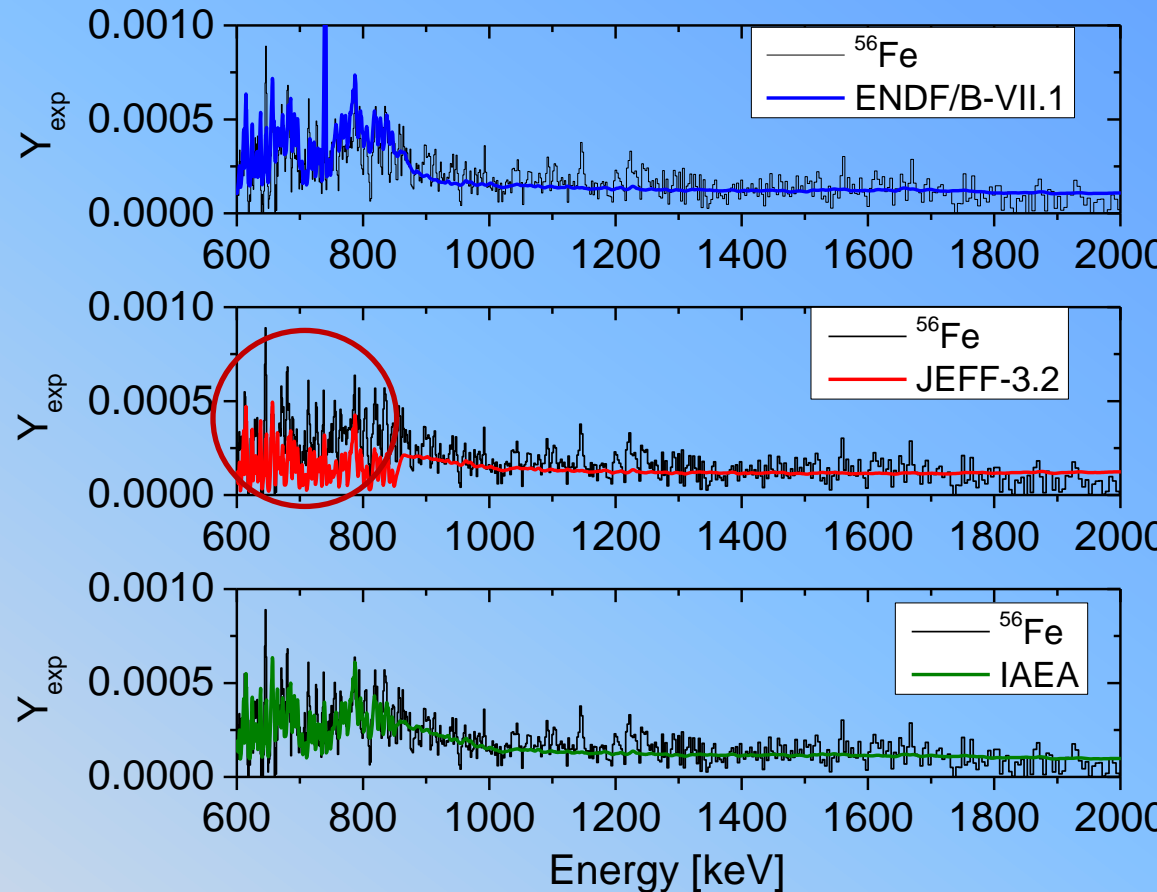
^{56}Fe Results – MCNP Comparison

- Evaluation comparisons among ENDF, JEFF and IAEA were performed using MCNP
- Background in ENDF is apparent above 400 keV
- Differences observed among resonances in the different evaluations



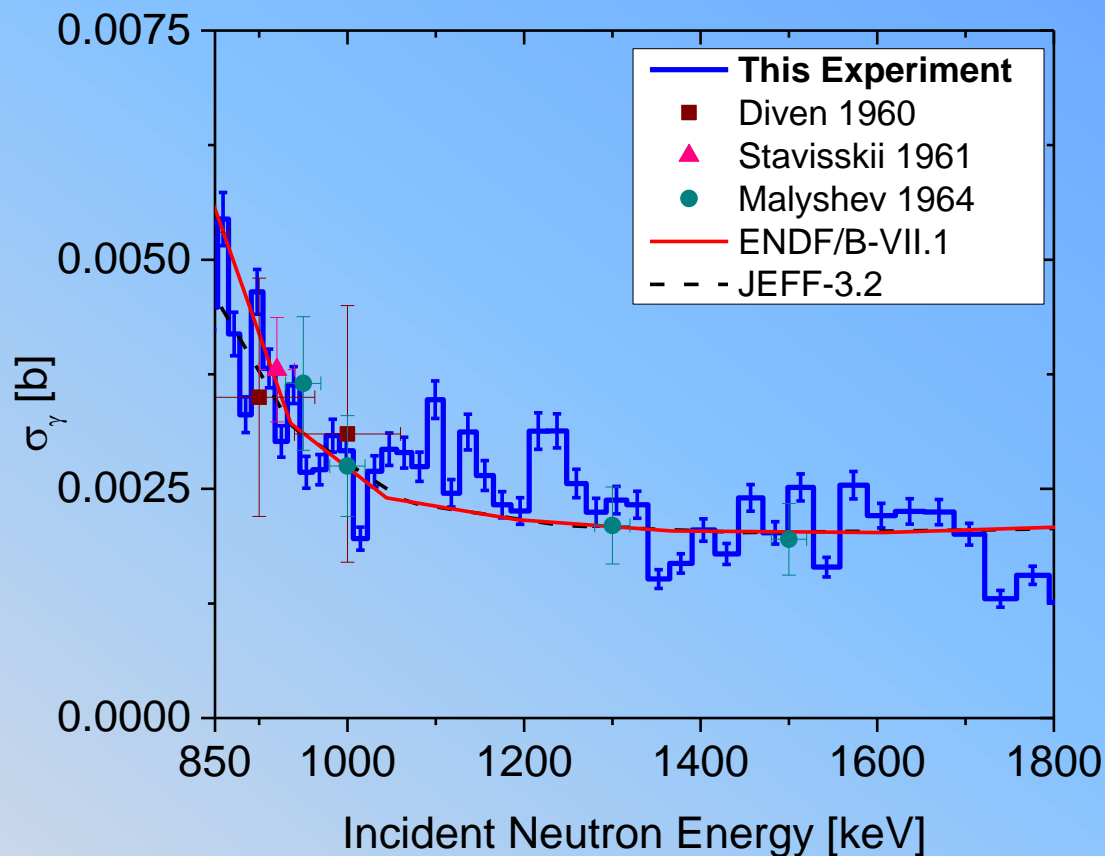
^{56}Fe Results – MCNP Comparison

- Possible unresolved or intermediate structure may account for higher data yields from 600-850 keV (self-shielding)
- ENDF overcompensates with its background treatment, JEFF has no background treatment.
- Above 850 keV, the data agree with the 3 evaluations presented.



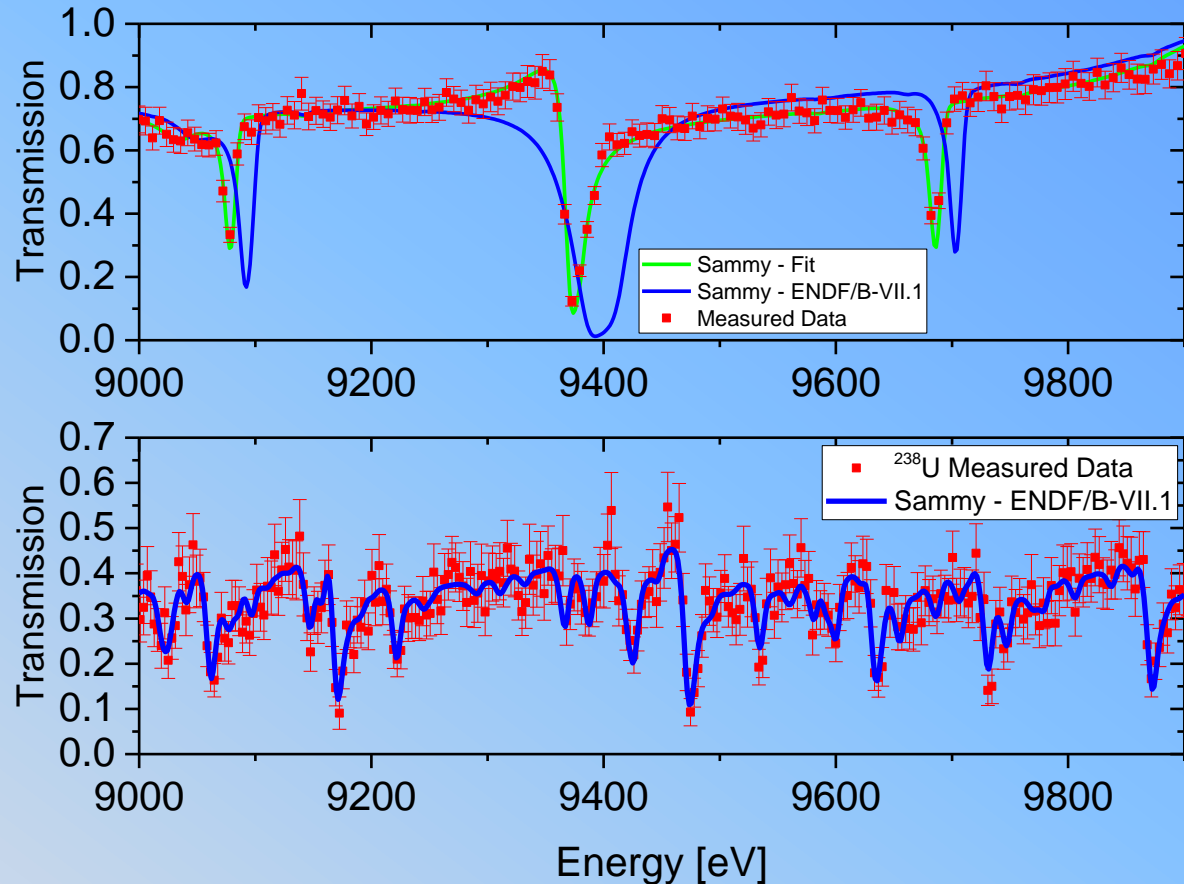
^{56}Fe Results – High Energy – other experiments

- High energy (>850 keV) data are in good agreement with previous experiments
- Data agree with ENDF and JEFF evaluations up to 1725 keV



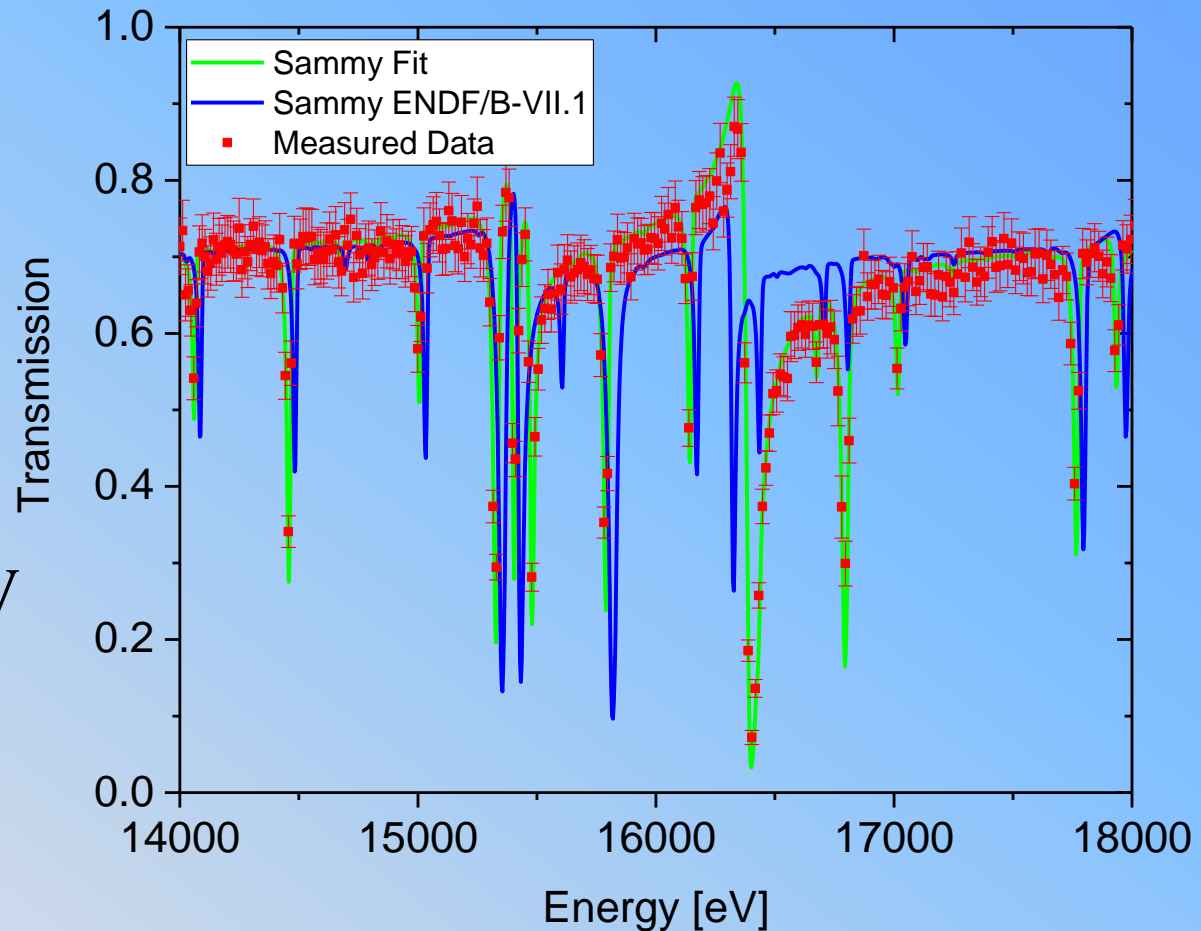
Mo-96 Transmission

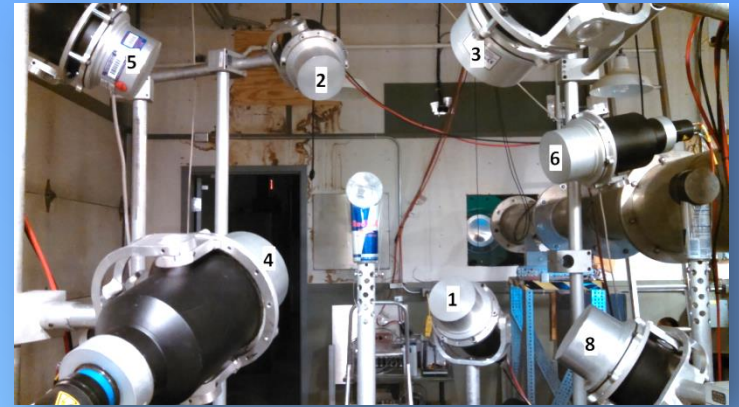
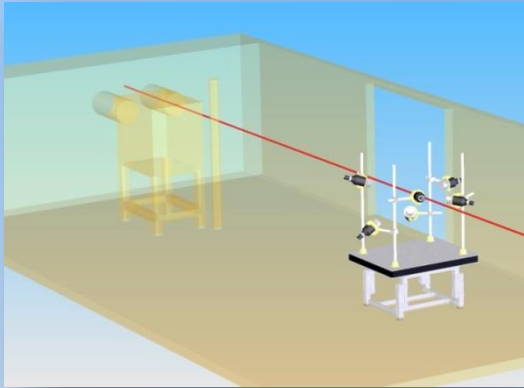
- Measurements included $^{95,96,98,100}\text{Mo}$
 - 100.141 m flight path
- Analysis of ^{96}Mo
 - 96.76% enriched
 - Areal density 0.05653 atoms/barn
- Use ^{238}U for energy alignment
 - Accurate determination of flight path and time zero.
 - Also used to verify the energy resolution used in SAMMY
- Observed
 - Energy shift in ^{96}Mo
 - Spin assignment problems (p-wave instead of s-wave)



Mo-96 Resonance Analysis up to 20 keV

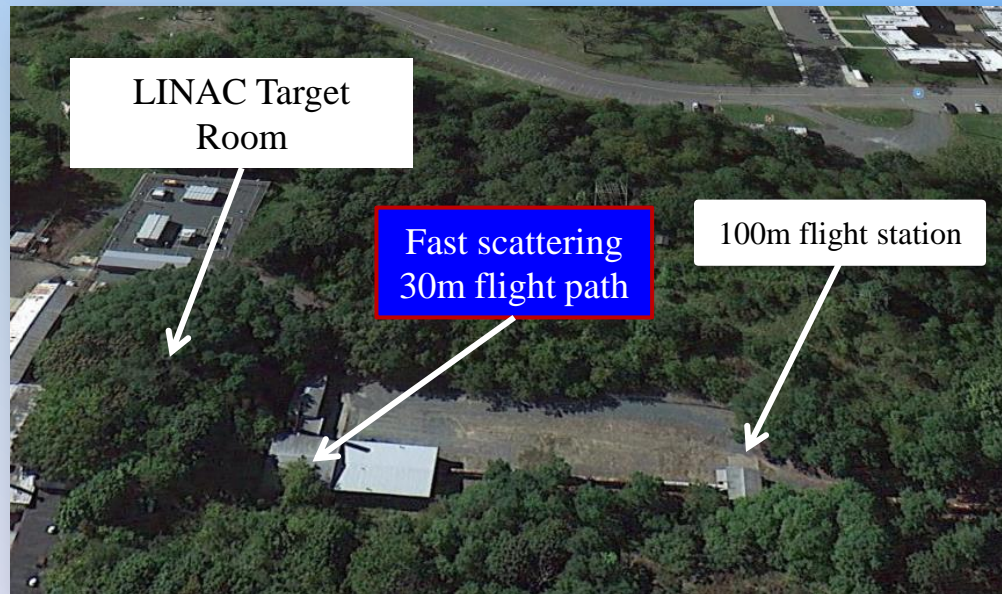
- Above 14 keV ENDF/B-VII.1 resonance parameters still shows
 - An energy shift
 - Issues with resonance parameters
- New resonance parameters from 5 keV to 30 keV were derived using the fitting code SAMMY





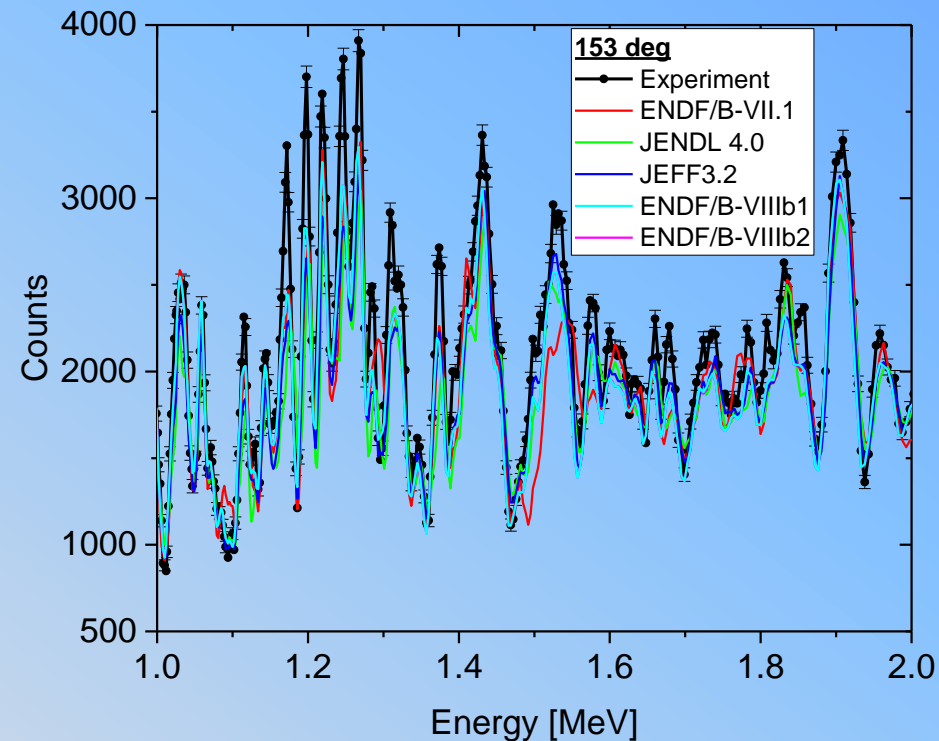
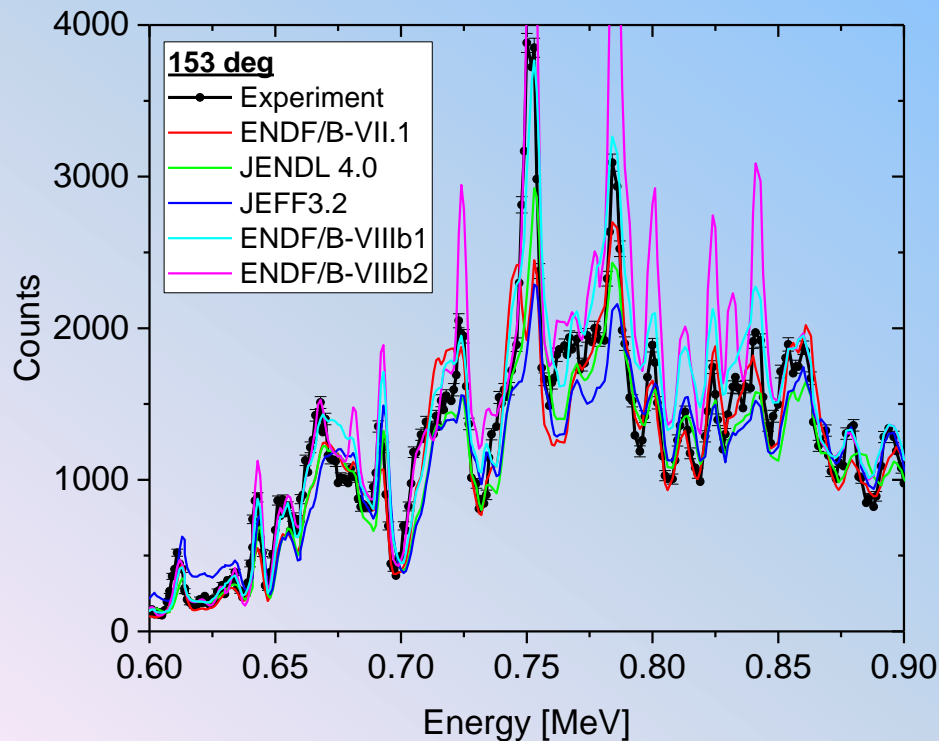
Neutron scattering benchmark of Fe-56 evaluations

Quasi-differential neutron scattering and angular distributions.



^{nat}Fe Scattering to 153 deg

- Left plot – energies below the 1st inelastic state (RRR region)
 - ENDF/B-VIIIb2 performs **very poorly** compared to other evaluations.
- Right Plot – above the first inelastic state (fast region)
 - ENDF/B-VIIIb2 and ENDF/B-VIIIb1 are same (b1 was plotted over b2)
- In order to quantify the differences FOM and C/E metrics were developed (next slides).



^{56}Fe FOM

- For this comparison we define for a given angle FOM as

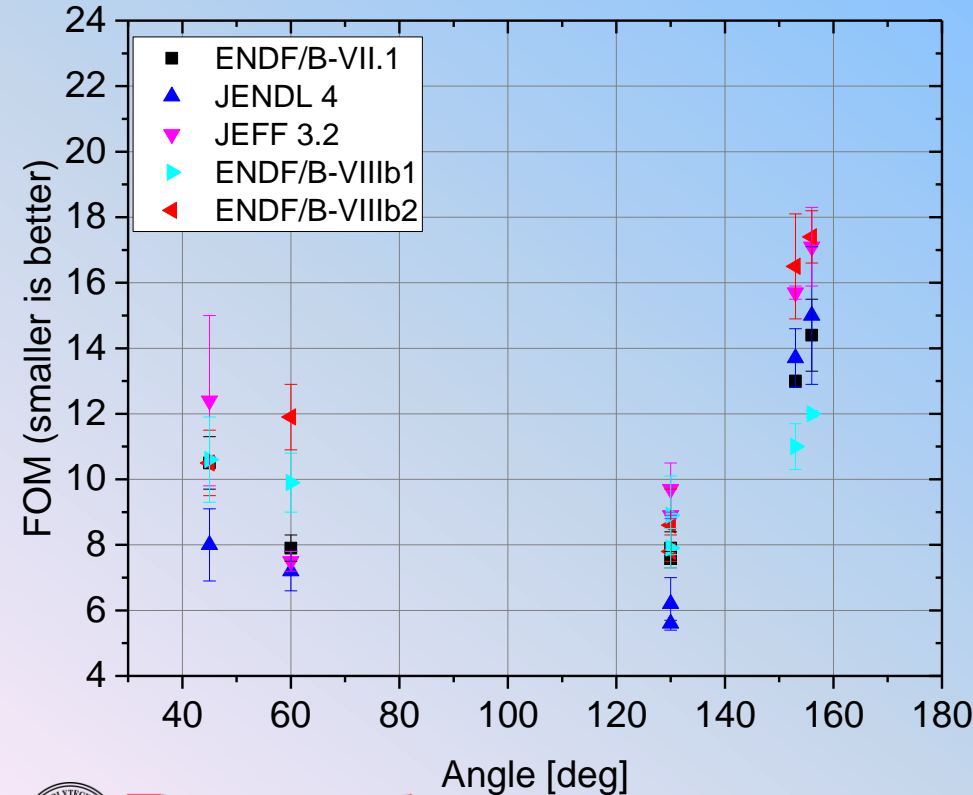
$$FOM = \frac{1}{n} \sum_{i=1}^n \frac{(Ex_i - Sim_i(1 \pm \epsilon_N))^2}{\Delta Ex_i^2 - (\epsilon_N Ex_i)^2}$$

n – number of TOF channels

Ex_i, Sim_i – Experimental net counts, and normalize net simulation results

ϵ_N – fractional normalization uncertainty

ΔEx_i - uncertainty in the measured net number of counts



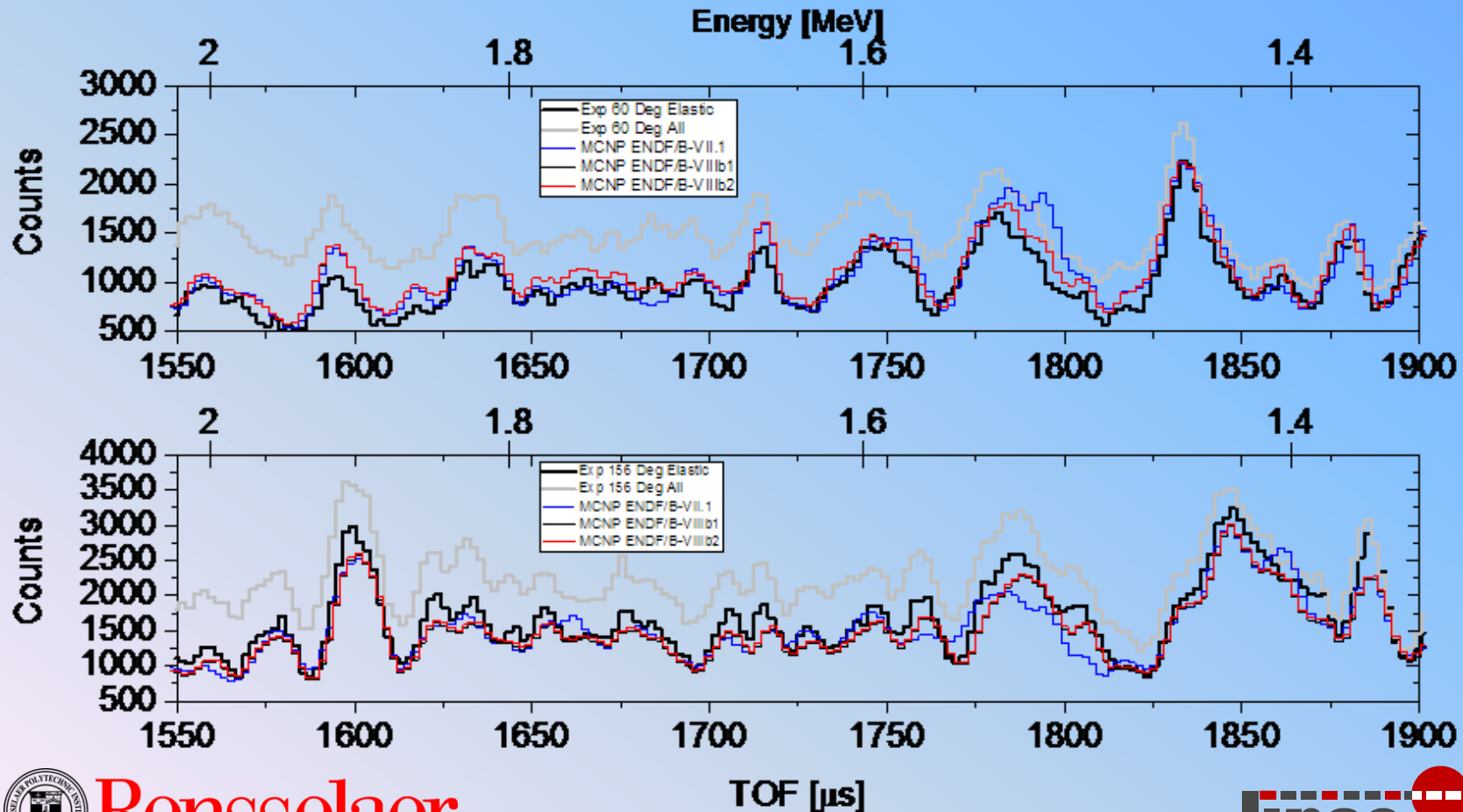
JENDL 4 is overall best (lowest FOM)

ENDF/B-VIIIb2 – performs poorly relative to other evaluations.

Table with numbers on next slide

^{56}Fe elastic scattering

- Remove inelastic neutron by discriminating their low pulse height.
- ENDF/B-VIIIb1 and b2 are the same and seem to follow the experimental data closer than ENDF/B-VII.1



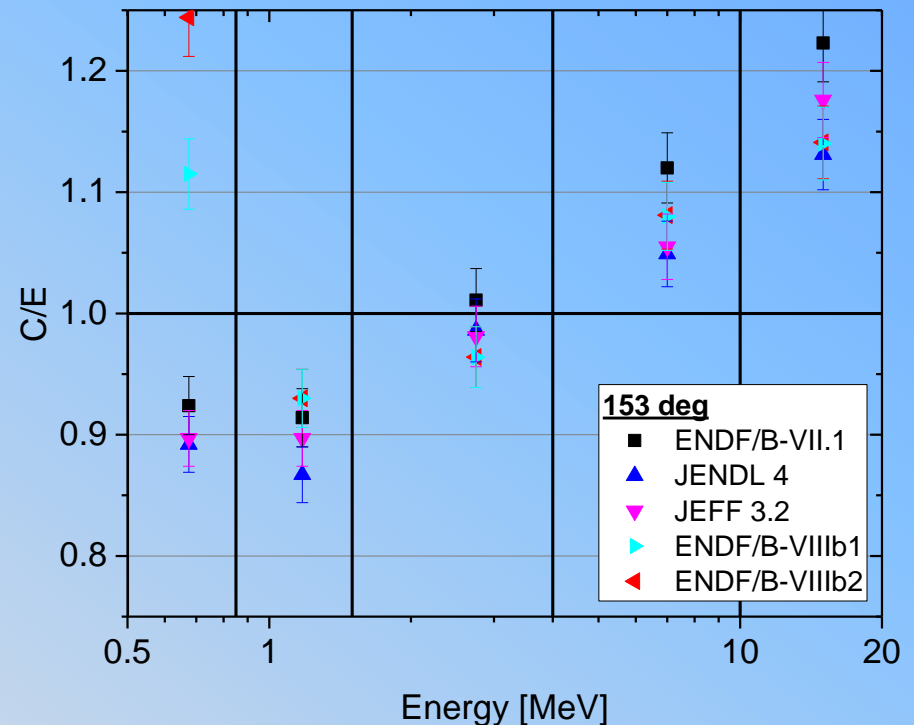
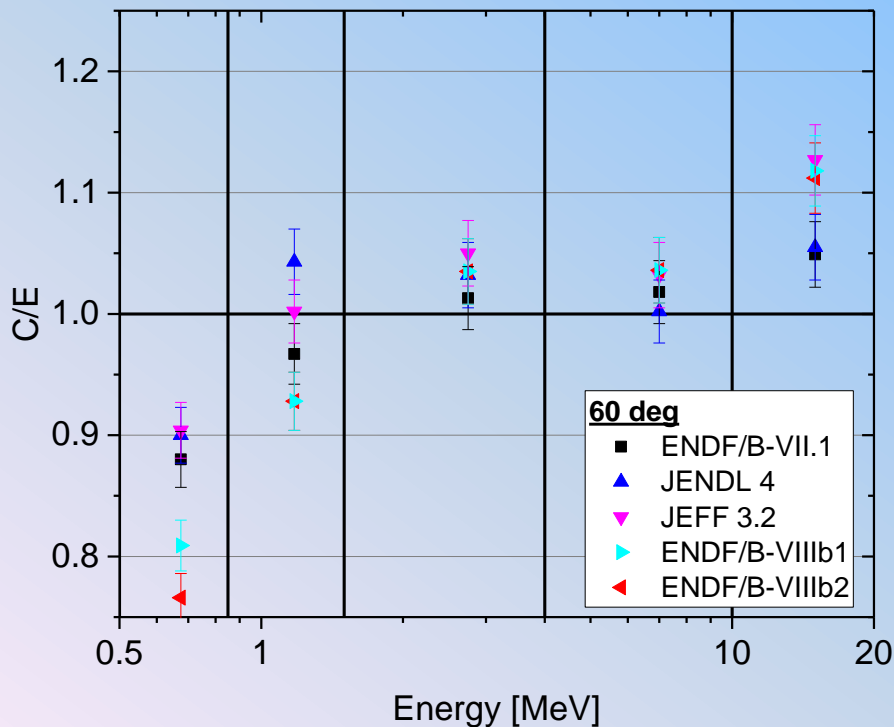
⁵⁶Fe FOM Table

- Lowest FOM was highlighted; however, it could be within uncertainty of neighboring FOM values.
- Note that the 156 deg data should be similar to the 153 deg data, but the FOMs are much larger, and so are the uncertainties due to normalization.

Angle	ENDF /B-VII.1	±	JENDL 4.0	±	JEFF 3.2	±	ENDF /B-VIIIb1	±	ENDF /B-VIIIb2	±
60	7.9	0.4	7.2	0.6	7.5	0.3	9.9	0.9	11.9	1.0
153	13.0	0.1	13.7	0.9	15.7	0.2	11.0	0.7	16.5	1.6
156	14.4	1.1	15.0	2.1	17.1	1.2	12.0	0.1	17.4	0.8
130	7.6	0.2	5.6	0.1	8.9	0.1	7.9	0.6	7.8	0.5
130	7.9	0.5	6.2	0.8	9.7	0.8	8.9	1.2	8.6	1.1
45	10.5	0.8	8.0	1.1	12.4	2.6	10.6	1.3	10.5	1.0

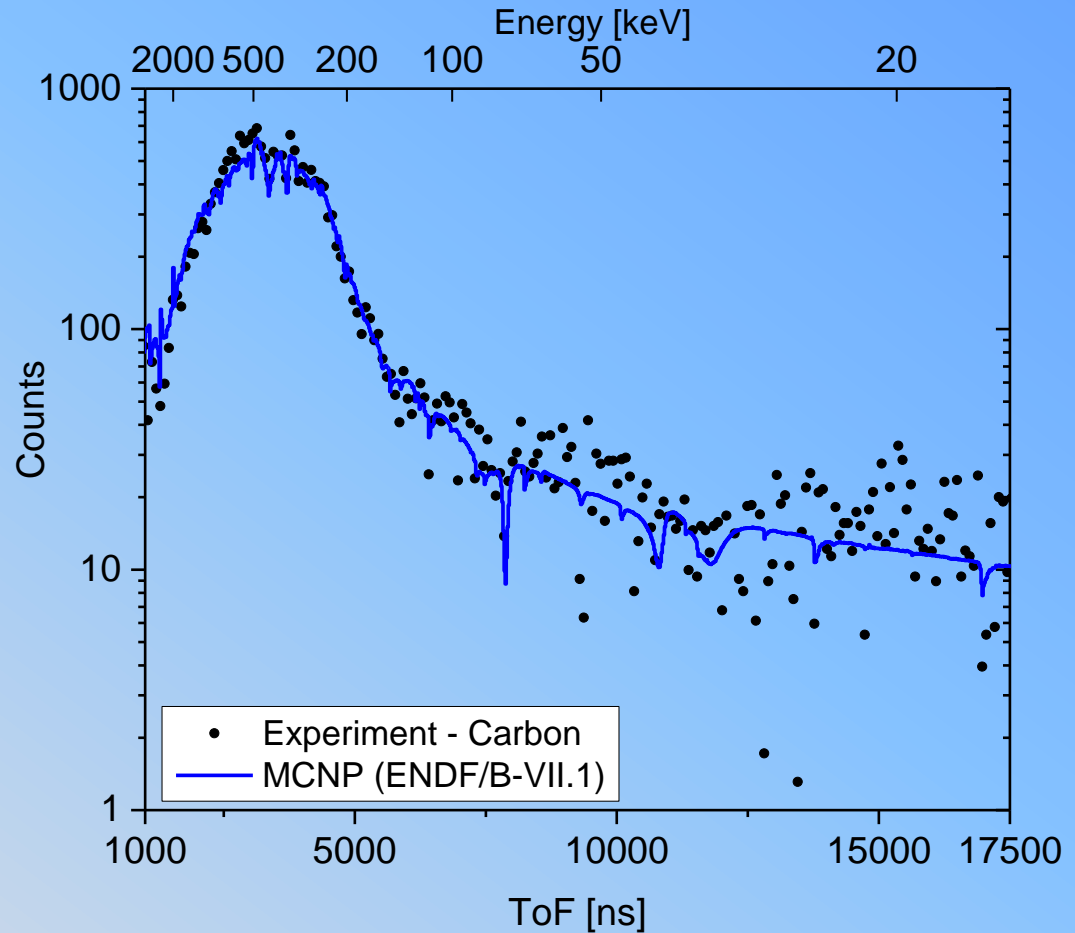
^{56}Fe C/E

- C/E was calculated by first grouping the data and calculating the group ratio
- The uncertainty includes only the simulation normalization uncertainty
- ENDF/B-VIIIb2 – performs poorly especially below 2 MeV.
- ENDF/B-VIIIb1 – shows slight improvement compared to ENDF/B-VII.1 for $E > 2$ MeV



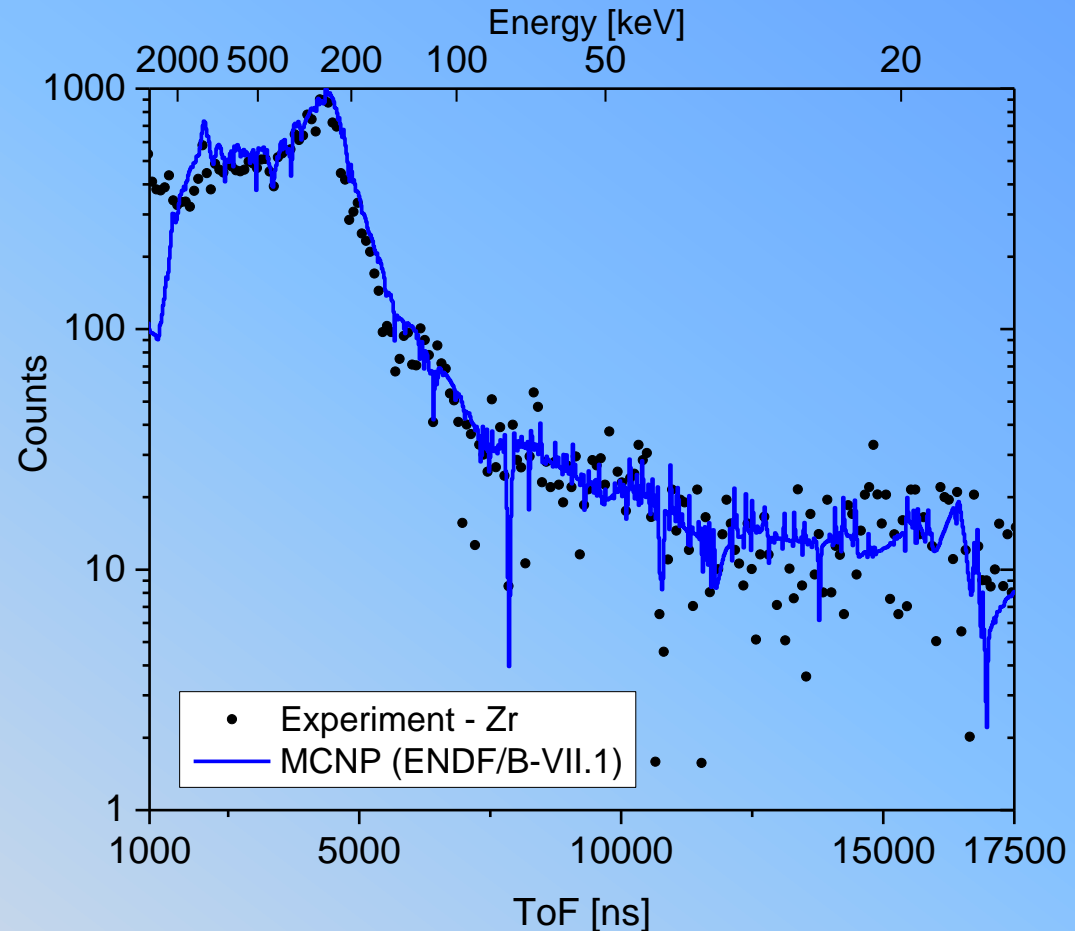
keV Region Scattering - Carbon

- **Objective:** supplement our fast (0.5-20 MeV) neutron scattering experiment with data below 0.5 MeV
 - Measure elastic/inelastic neutron scattering as several angles
- Carbon (graphite) was used for validation of the methodology
 - Structure in the data (dips) due to transmission through Al in the beam
- Neutron scattering from a 7 cm carbon sample was measured with a 1 inch diameter by 0.5 inch thick ^6Li detector at 45 degrees
 - Experiment and simulation show good agreement above 100 keV
 - Counting statistics need improvement



keV Region Scattering - Zr

- Neutron scattering from a 4 cm thick zirconium sample was measured with a 1 inch diameter by 0.5 inch thick ^6Li detector at 45 degrees
- Below 500 keV, good agreement was found between the measurement and simulation
- Improvements include:
 - Larger detector area (3" diam.)
 - Two detectors at the same angle
 - Improve counting statistics with a longer run time.
 - Used ~9 hours for the sample and ~3 hours for the open.



Summary

- **Results presented**
 - RRR (capture/transmission) : $^{161,162,163,164}\text{Dy}$, Rh, Fe, ^{56}Fe
 - URR capture: Fe, ^{56}Fe
 - $^{\text{nat}}\text{Fe}$ neutron scattering
 - keV scattering from C and Zr.
- **Planned/in progress measurements**
 - Zr - keV scattering
 - Hf - Transmission and scattering
 - Ta - Transmission and capture in the RRR
 - Be, Ta photoneutron production